Anal. Chem. **2003,** *75,* 6995−7007

Radiolytic Modification of Basic Amino Acid Residues in Peptides: Probes for Examining Protein−Protein Interactions

Guozhong Xu,[†,‡] Keiji Takamoto,[†,‡] and Mark R. Chance*[,†,‡,§]

Department of Physiology & Biophysics, Department of Biochemistry, and Center for Synchrotron Biosciences, Albert Einstein College of Medicine, 1300 Morris Park Avenue, Bronx, New York 10461-1602

Protein footprinting utilizing hydroxyl radicals coupled with mass spectrometry has become a powerful technique for mapping the solvent accessible surface of proteins and examining protein−protein interactions in solution. Hydroxyl radicals generated by radiolysis or chemical methods efficiently react with many amino acid residue side chains, including the aromatic and sulfur-containing residues along with proline and leucine, generating stable oxidation products that are valuable probes for examining protein structure. In this study, we examine the radiolytic oxidation chemistry of histidine, lysine, and arginine for comparison with their metal-catalyzed oxidation products. Model peptides containing arginine, histidine, and lysine were irradiated using white light from a synchrotron X-ray source or a cesium-137 γ-ray source. The rates of oxidation and the radiolysis products were primarily characterized by electrospray mass spectrometry including tandem mass spectrometry. Arginine is very sensitive to radiolytic oxidation, giving rise to a characteristic product with a 43 Da mass reduction as a result of the loss of guanidino group and conversion to γ-glutamyl semialdehyde, consistent with previous metal-catalyzed oxidation studies. Histidine was oxidized to generate a mixture of products with characteristic mass changes primarily involving rupture of and addition to the imidazole ring. Lysine was converted to hydroxylysine or carbonylysine by radiolysis. The development of methods to probe these residues due to their high frequency of occurrence, their typical presence on the protein surface, and their frequent participation in protein−protein interactions considerably extends the utility of protein footprinting.

Hydroxyl radical mediated footprinting of proteins coupled to mass spectrometry analysis has emerged as a powerful technique for mapping the solvent accessible surface of proteins, allowing both protein structure as well as the direct and allosteric interactions of protein with ligands to be explored in detail.[1−11] Hydroxyl radicals can be generated by a number of means, and various methods to modify accessible and reactive protein side chains including radiolysis,[1,3,5−7,10,12,13] Fenton reagents,[8] and electrical discharge[9,14] have been recently developed in order to probe protein structure. The radiolysis of water has a number of advantages as a radical source including no need for added reagents, a wide range of possible solution conditions can be used, and control of the total dose can be quite precise. We have used synchrotron X-ray beamlines at the National Synchrotron Light Source (NSLS) of Brookhaven National Laboratory as a source of radicals for the development of radiolytic footprinting for both nucleic acid and protein footprinting experiments.[5,13,15−17] Exposure of nucleic acid and protein samples to a synchrotron white beam for tens of milliseconds provides sufficient cleavage of nucleic acids or modification of proteins for structural mapping. Combined with rapid mixing techniques, radiolytic footprinting is a powerful approach for investigating the dynamic processes of macromolecules,[16−18] particularly RNA folding and DNA−protein interactions.[15,19−21] However, synchrotron access is nontrivial, and high flux sources are necessary only for time-resolved experiments. Irradiation of aqueous solutions with various forms of radiation such as γ-rays, β-particles, or fast neutrons results in similar ionizations of water. Protein footprinting with low flux radiolysis sources should provide results similar to those with

* Corresponding author. Telephone: (718)430-4136. Fax: (718)430-8587. E-mail: mrc@aecom.yu.edu.

† Department of Physiology & Biophysics.

‡ Center for Synchrotron Biosciences.

§ Department of Biochemistry.

(1) Kiselar, J. G.; et al. *Proc. Natl. Acad. Sci. U.S.A.* **2003**, *100* (7), 3942−7.
(2) Kiselar, J. G.; et al. *Int. J. Radiat. Biol.* **2002**, *78* (2), 101−14.
(3) Goldsmith, S. C.; et al. *J. Biomol. Struct. Dyn.* **2001**, *19* (3), 405−18.
(4) Rashidzadeh, H.; et al. *Biochemistry* **2003**, *42* (13), 3655−65.
(5) Guan, J. Q.; et al. *Biochemistry* **2002**, *41* (18), 5765−75.
(6) Guan, J. G.; et al. *Biochemistry* **2003**, *42* (41), 11992-2000.
(7) Liu, R.; et al. *Biochemistry* **2003**, *42* (43), 12447−54.
(8) Sharp, J. S.; Becker, J. M.; Hettich, R. L. *Anal. Biochem.* **2003**, *313* (2), 216−25.
(9) Wong, J. W.; Maleknia, S. D.; Downard, K. M. *Anal. Chem.* **2003**, *75* (7), 1557−63.
(10) Chance, M. R. *Biochem. Biophys. Res. Commun.* **2001**, *287* (3), 614−21.
(11) Kiselar, J. G.; et al. *Mol. Cell. Proteomics* **2003**, *2* (10), 1120−1132.
(12) Maleknia, S. D.; Brenowitz, M.; Chance, M. R. *Anal. Chem.* **1999**, *71* (18), 3965−73.
(13) Maleknia, S. D.; et al. *Anal. Biochem.* **2001**, *289* (2), 103−15.
(14) Maleknia, S. D.; Chance, M. R.; Downard, K. M. *Rapid Commun. Mass. Spectrom.* **1999**, *13* (23), 2352−8.
(15) Sclavi, B.; et al. *Science* **1998**, *279* (5358), 1940−3.
(16) Sclavi, B.; et al. *Methods Enzymol.* **1998**, *295*, 379−402.
(17) Chance, M. R.; et al. *Structure* **1997**, *5* (7), 865−9.
(18) Ralston, C. Y.; et al. *Methods Enzymol.* **2000**, *317*, 353−68.
(19) Rangan, P.; et al. *Proc. Natl. Acad. Sci. U.S.A.* **2003**, *100* (4), 1574−9.
(20) Uchida, T.; et al. *J. Mol. Biol.* **2003**, *328* (2), 463−78.
(21) Dhavan, G. M.; et al. *J. Mol. Biol.* **2002**, *315* (5), 1027−37.

10.1021/ac035104h CCC: $25.00
Published on Web 11/07/2003

synchrotron X-rays except that longer time scales of seconds to minutes instead of milliseconds is anticipated. In fact in the case of nucleic acid footprinting, this has been demonstrated to be the case.[22,23]

The hydroxyl radicals generated through the above methods can efficiently oxidize amino acids on or near the surface of proteins in direct relation to their reactivity and their solvent accessibility.[2,3,5,8,9,11] In particular, the solvent-accessible side chains of cysteine, methionine, phenylalanine, tyrosine, tryptophan, histidine, proline, and leucine provide convenient and useful probes for protein footprinting.[8,10−13] Since, these residues cover 25−30% of the sequence of a typical protein (http://prowl.rockefeller.edu/),[24] many sites throughout a protein's structure are potential probes for the method. Hydroxyl radical mediated footprinting mass spectrometry (MS) is very similar to deuterium exchange MS methods[25−27] except that the side chains instead of backbone positions are probed, and the covalent nature of the modifications permits the application of a wide variety of proteases, chromatographic separations, and tandem MS approaches in order to interrogate structure. Briefly, protein samples are subjected to oxidation by any one of the methods outlined above. Following digestion of oxidized protein solutions with proteases, the digests are typically separated by reversed-phase liquid chromatography and analyzed by electrospray ionization (ESI) or directly analyzed by matrix-assisted laser desorption (MALDI) MS methods. To measure specific rates of oxidation for a peptide, the amounts of modified and unmodified peptide are individually quantitated for a specific exposure time, and the rate of oxidation of peptides containing the susceptible sites is determined by several measurements at varying exposure times.[2,3,5] It should be noted that protein footprinting using side-chain modification has a venerable history, a number of reagents to specifically modify protein side chains were developed in the 1960s and 1970s, and these were even proposed as possible methods to map amino acids that were on the protein surface versus those that were buried.[28] Specific footprinting protocols to map surfaces using covalent modification were introduced by Hanai and Wang.[29] In this case, modification of surface-accessible lysine residues was used as a probe of protein−DNA interactions. These studies emphasized the specific protocols that must be adhered to for footprinting experiments to report biochemically and biophysically appropriate data.[28,30]

Three features of radiolytic footprinting as developed in this laboratory ensure that the intact population of molecules is probed; such safeguards are the hallmark of all footprinting approaches, which depend on the covalent modification or cleavage of macromolecules to probe the structure.[28,30] First, the rate of loss of the unmodified fraction is examined, emphasizing the disappearance of biologically intact material. Second, the total dose is limited, and third, the observation of a first-order process in the loss of the unmodified fraction ensures that no dose-dependent changes in reactivity are induced by the oxidations. The rates of oxidation for specific peptides are analyzed in the context of structural data when available. Such data allow the explicit solvent accessibility of the side chains of interest to be calculated or in the context of structural models if 3-D coordinates are not available. The power of the method is most apparent in examining the changes in structure upon ligand binding since the oxidation rates of a particular peptide site may increase, decrease, or stay the same in response to ligand binding. Each of these possible results is informative.

Hydroxyl radicals react preferentially with the side chains of amino acid residues due to the steric hindrance of main-chain α-carbon under typical radiolysis conditions.[31−33] One reason is that the main-chain α-carbon is shielded, especially when bulky side-chain groups are present. Another reason is the difficulty of α-carbon radicals to achieve a planar trigonal configuration for its three attached groups. The oxidation is also preferred at sites where the radical will be stabilized by neighboring functional groups such as unsaturated bonds or electron-rich heteroatoms through electron delocalization and to a lesser degree by electron-releasing alkyl groups through electron donation to the electron-deficient radical centers.[31−35] This explains why oxidation at aromatic and sulfur-containing amino acid residues has been easily observed in the peptide and protein footprinting studies to date.[5,8,12] Direct measurements of the oxidation rates of different amino acid residues by hydroxyl radicals have been determined by pulse radiolysis and optical spectroscopy.[36] Table 1 lists the rates of reaction of hydroxyl radicals with the 20 common amino acids; the amino acids are shown in order of their rate of reaction with hydroxyl radicals. For a particular side chain within a peptide, the observed rate of oxidation depends on the relative reactivity as well as the solvent accessibility of the side-chain residue. The residues typically used in protein footprinting experiments are well-represented among the most reactive residues listed. As stated above, the side chains typically used in protein footprinting experiments cover more than 25% of the typical protein's sequence. Extension of the typical set of side chains that can be analyzed would expand the sequence coverage in proportion to the frequency of occurrence of the side chains. Thus, the "next" most reactive residues in Table 1 represent logical probes for expanding the method.

The value of a side chain as a probe of protein−ligand interactions also depends on its degree of solvent accessibility. Table 1 presents the average probability of a side-chain residue having a solvent-accessible area ≥30 Å^2, which is a reasonable threshold for being easily oxidized under typical footprinting

(22) Franchet-Beuzit, J.; et al. *Biochemistry* **1993**, *32* (8), 2104−10.
(23) Tullius, T. D.; et al. *Methods Enzymol.* **1987**, *155*, 537−58.
(24) Fenyo, D.; et al. *Anal. Chem.* **1996**, *68*, 721A−726A.
(25) Katta, V.; Chait, B. T. *J. Am. Chem. Soc.* **1993**, *115*, 6317−6321.
(26) Zhang, Z.; Smith, D. L. *Protein Sci.* **1993**, *2* (4), 522−31.
(27) Hoofnagle, A. N.; Resing, K. A.; Ahn, N. G. *Annu. Rev. Biophys. Biomol. Struct.* **2003**, *32*, 1−25.
(28) Guan, J. Q.; Chance, M. R. Footprinting Methods to Examine the Structure and Dynamics of Proteins. In *Encyclopedia of Molecular Cell Biology and Molecular Medicine*, 2nd ed.; Meyers, R., Ed.; Wiley Inc.: New York, 2003.
(29) Hanai, R.; Wang, J. C. *Proc. Natl. Acad. Sci. U.S.A.* **1994**, *91* (25), 11904−8.
(30) Takamoto, K.; Chance, M. Footprinting Methods to Examine the Structure and Dynamics of Nucleic Acids. In *Encyclopedia of Molecular Cell Biology and Molecular Medicine*, 2nd ed.; Meyers, R., Ed.; Wiley Inc.: New York, 2003.
(31) Hawkins, C. L.; Davies, M. J. *J. Chem. Soc., Perkin Trans. 2* **1998**, 2617−22.
(32) Hawkins, C. L.; Davies, M. J. *Biochim. Biophys. Acta* **2001**, *1504* (2−3), 196−219.
(33) Davies, M. J.; Dean, R. T. *Radical-mediated protein oxidation: from chemistry to medicine*; Oxford University Press; Oxford, 1997.
(34) Garrison, W. M. *Chem. Rev.* **1987**, *87*, 381−98.
(35) Stadtman, E. R. *Methods Enzymol.* **1995**, *258*, 379−93.
(36) Buxton, G. V.; et al. *J. Phys. Chem. Ref. Data* **1988**, *17*, 513−886.

Table 1. Amino Acid Data

amino acid	rate of reaction with •OH (M^{-1} s^{-1})[a]	frequency in proteins (%)[b]	fraction observed with SEA >30 Å^2 [c]	SEA × frequency[d]
Cys	3.4×10^{10}	2.8	0.32	0.9
Tyr	1.3×10^{10}	3.5	0.67	2.3
His	1.3×10^{10}	2.1	0.66	1.4
Met	8.3×10^{9}	1.7	0.44	0.7
Phe	6.5×10^{9}	3.5	0.42	1.5
Arg	3.5×10^{9}	4.7	0.84	3.9
Leu	1.7×10^{9}	7.5	0.41	3.1
Ile	na	4.6	0.39	1.8
Trp	1.3×10^{9}	1.1	0.49	0.5
Pro	na	4.6	0.78	3.6
Val	7.6×10^{8}	6.9	0.4	2.8
Thr	5.1×10^{8}	6.0	0.71	4.3
Ser	3.2×10^{8}	7.1	0.70	5.0
Glu	2.3×10^{8}	6.2	0.93	5.8
Gln	na	3.9	0.81	3.2
Ala	7.7×10^{7}	9.0	0.48	4.3
Asp	7.5×10^{7}	5.5	0.81	4.5
Asn	4.9×10^{7}	4.4	0.82	3.6
Lys	3.5×10^{7}	7.0	0.93	6.5
Gly	1.7×10^{7}	7.5	0.51	3.8

[a] The bimolecular rate constants of formation with hydroxyl radicals for the 20 amino acids.[36] na means not available in the literature. [b] Average occurrence frequency of 20 amino acids in proteins. [c] Average probability of 20 amino acid side chains having a surface-exposed area (SEA) ≥30 Å^2 (http://prowl.rockefeller.edu). [d] Frequency of occurrence multiplied by probability of SEA ≥30 Å^2.

conditions.[2] This probability is calculated based on examination of 55 entries from the Brookhaven Protein Database, and although it may not extend to all proteins, the results are intuitively reasonable (http://prowl.rockefeller.edu).[24] Obviously, charged residues are very frequently found on the surface of proteins (e.g., Lys and Glu, 93%), but hydrophobic residues frequently have significant solvent accessibility as well, with Tyr at 67% and Trp at 49%. Multiplication of the frequency of occurrence in percent times the fraction of surface accessible gives a relative value of the usefulness, on average, of various side-chain probes in surface mapping (footprinting) experiments. Of the residues in use currently, Pro at 3.6 and Leu at 3.1 are in many ways the most valuable. But, based on this assumption, the basic and acidic residues (such as Arg, Lys, Asp, and Glu) are potentially very useful probes for mapping the protein surface.

Systematic statistical analyses of protein−protein interfaces reveal that charged and polar amino acids exist in protein interfaces less frequently than on the protein surface in general, but they are more frequently found in interfaces than in the protein interior.[37,38] Although the hydrophobic effect still plays the most significant role in protein−protein interactions, hydrogen bonds and ion pairs are very important for protein−protein binding. The charged interactions are very important for binding specificity[39−41] and rapid binding kinetics[42] due to the long-range electrostatic steering effect. Arginine ranks second in frequency of occurrence among the most common amino acids found in interfaces (the top three are Trp, Arg, and Tyr), likely due to its capacity for multiple types of favorable interactions.[43] It is able to form up to five H-bonds and a salt-bridge through the positively charged guanidino group as well as hydrophobic interactions because of the pseudo-aromatic character of electron-delocalized guanidino π-system and the three hydrophobic methylene carbon atoms. Of course arginine and lysine also play key roles in protein−nucleic acid recognition and interactions.[44−46]

The value implied in the utilization of additional probes is balanced by the lower reactivity for some of the residues and the likely attendant difficulty in detecting their oxidation. However, Arg is apparently twice as reactive as Leu, so the failure to observe it in experiments to date requires some explanation. Nevertheless, an extension of the footprinting approach to positively charged side chains would permit the specific detection of electrostatically driven protein−ligand interactions, which are commonly seen upon protein−nucleic acid binding as well as in protein complexes.

To utilize side-chain modification for radiolytic footprinting experiments and to expand the set of probe residues, a detailed understanding of the radiolytic chemistry of oxidation of the amino acid residues is required. Fortunately, over 40 yr of extensive research has addressed a number of the relevant questions. Oxidation of aliphatic side chains with hydroxyl radicals in the presence of O_2 can generate hydroperoxide, alcohol, and carbonyl products through initial hydrogen atom abstraction and further reaction with O_2.[31−35,47,48] The unstable peroxides decompose quickly in the presence of heat, light, reductants, or metal ions. Overall, the oxidized products show a mass change of +16 Da for formation of alcohol groups or +14 Da for formation of carbonyl groups. However, oxidation of heteroatom-containing side chains may cause further cleavage of side chains and generate unique products with observed mass changes other than +14 or +16 Da.[31−35,47,48] For instance, oxidation of arginine by metal ion-catalyzed oxidation (MCO) systems has been reported to produce γ-glutamyl semialdehyde due to the loss of guanidino group.[49−56] A similar oxidation is expected to take place in the case of radiolysis, although this has not been reported to date. In the case of aromatic residues (Phe, Tyr, Trp, and His), the radicals attack almost exclusively on the aromatic rings resulting in oxidative ring addition and even ring scission in the case of Trp and His, producing a range of complex products.[35]

In this work, we focus on examining the radiolytic oxidation mechanisms of arginine, histidine, and lysine to explore their suitability as probes for protein footprinting, both to expand the coverage of the protein sequence and to enhance our ability to monitor protein−ligand interactions. We identify multiple but

(37) Tsai, C. J.; et al. *Protein Sci.* **1997**, *6* (1), 53−64.
(38) Xu, D.; Lin, S. L.; Nussinov, R. *J. Mol. Biol.* **1997**, *265* (1), 68−84.
(39) Lee, L. P.; Tidor, B. *Nat. Struct. Biol.* **2001**, *8* (1), 73−6.
(40) O'Shea, E. K.; Rutkowski, R.; Kim, P. S. *Cell* **1992**, *68* (4), 699−708.
(41) Riordan, J. F.; McElvany, K. D.; Borders, C. L., Jr. *Science* **1977**, *195* (4281), 884−6.
(42) Schreiber, G.; Fersht, A. R. *Nat. Struct. Biol.* **1996**, *3* (5), 427−31.
(43) Bogan, A. A.; Thorn, K. S. *J. Mol. Biol.* **1998**, *280* (1), 1−9.
(44) Calnan, B. J.; et al. *Science* **1991**, *252* (5010), 1167−71.
(45) Ibba, M.; Soll, D. *Nature* **1996**, *381* (6584), 656.
(46) Jones, S.; et al. *J. Mol. Biol.* **1999**, *287* (5), 877−96.
(47) Stadtman, E. R. *Annu. Rev. Biochem.* **1993**, *62*, 797−821.
(48) Klapper, M. H.; Faraggi, M. *Q Rev. Biophys.* **1979**, *12* (4), 465−519.
(49) Davies, M. J.; et al. *Free Radical Biol. Med.* **1999**, *27* (11−12), 1151−63.
(50) Amici, A.; et al. *J. Biol. Chem.* **1989**, *264* (6), 3341−6.
(51) Climent, I.; Tsai, L.; Levine, R. L. *Anal. Biochem.* **1989**, *182* (2), 226−32.
(52) Ayala, A.; Cutler, R. G. *Free Radical Biol. Med.* **1996**, *21* (1), 65−80.
(53) Ayala, A.; Cutler, R. G. *Free Radical Biol. Med.* **1996**, *21* (4), 551−8.
(54) Pietzsch, J. *Biochem. Biophys. Res. Commun.* **2000**, *270* (3), 852−7.
(55) Pietzsch, J.; Julius, U. *FEBS Lett.* **2001**, *491* (1−2), 123−6.
(56) Requena, J. R.; et al. *Proc. Natl. Acad. Sci. U.S.A.* **2001**, *98* (1), 69−74.

characteristic oxidation products for these residues consistent with known mechanisms of metal-catalyzed oxidation. We also validate the use of low-flux radiolysis sources (in this case γ-rays from a cesium source) as a means of generating hydroxyl radicals for footprinting for cases where use of Fenton reagents is undesirable.[8]

EXPERIMENTAL PROCEDURES

Materials. Peptides Ala-Arg-Arg-Ala (ARRA), Asp-Ala-His-Lys (DAHK), Asp-Ser-Asp-Pro-Arg (DSDPR), Gly-Phe-Gly (GFG), Lys-Arg-Ser-Arg (KRSR), Thr-Arg-Lys-Arg (TRKR), bradykinin (RPPGFSPFR), Gly-Arg-Ala-Asp-Ser-Pro-Lys (GRADSPK), Arg-Arg-Glu-Glu-Glu-Thr-Glu-Glu-Glu (RREEETEEE), calfluxin (RVDSADESNDDGFD), and human cytomegalovirus protease substrate M-site (RGVVNASSRLAK) were purchased from Bachem California Inc. (Torrance, CA). Myosin kinase inhibiting peptide (KKRAARATS-NH_2) was ordered from SynPep (Dublin, CA). All peptides had a purity at least of 95% except Asp-Ser-Asp-Pro-Arg, which had a purity of 91%. Hexafluoro-2-propanol (HFIP, 99% purity), Purpald, and NaOH were purchased from Aldrich (Milwaukee, MI). Trifluoroacetic acid (TFA) was sequencing grade reagent from Pierce Biotechnology Inc. (Rockford, IL). B&J Brand high-purity methanol and acetonitrile (MeCN) were purchased from Honeywell International Inc. (Muskegon, MI). Solutions of peptides at a concentration of 20 or 40 μM were prepared in Nanopure water using a Millipore Ultrapure Water System.

Exposure of Peptides to Radiation. The peptide solutions were exposed to either synchrotron X-rays at the X-28C beamline of NSLS at Brookhaven National Laboratory or a cesium-137 γ-ray source (3000 rad/min) at the Albert Einstein College of Medicine. Samples were exposed at beamline X-28C using the stand and shutter in a 5- (for ARRA) or 20-μL volume (for DAHK) of peptide solutions in 0.2-mL Eppendorf tubes. These samples were irradiated for 10−30 ms at beam currents ranging from 180 to 290 mA in accordance with our established protocols.[5,18] For samples exposed to the cesium-137 source, a 20-μL peptide solution in a 1.5-mL Eppendorf tube was exposed for 0.5−8.0 min, and the exposure time was also controlled by an electronic shutter. After exposure to radiation, all peptide samples were stored at −20 °C before mass spectroscopic analysis.

Mass Spectrometric Analysis of Peptides. The radiolytically oxidized peptides were analyzed directly by electrospray MS without chromatographic separation. The peptide concentrations were adjusted to 10 μM with methanol or acetonitrile and were infused directly into the ESI-MS at a flow rate of 3 μL/min. Mass spectra were acquired on a Finnigan LCQ quadrupole ion trap mass spectrometer (Finnigan Corp., San Jose, CA). The needle voltage was set at 4.5 kV. The instrument was tuned using the known masses of the unmodified peptides. Both positive and negative spectra were recorded in the profile mode as indicated in the results. To determine the sites of amino acid oxidation, the CID (collision-induced dissociation) MS/MS spectra and even MS/MS/MS spectra were acquired for the selected ions as previously described.[2,5,12]

An oxidized peptide, bradykinin, was also analyzed by HPLC-negative-ESI-MS. The sample was separated using an Alliance 2690 Waters (Milford, MA) HPLC system with a Vydac (Hesperia, CA) 1.0 × 150 mm reversed-phase C18 column at a flow rate of 50 μL/min. The solvent A contained 95% water, 5% MeCN, 0.05% TFA, and 20 mM HFIP, while the solvent B contained 5% water, 95% MeCN, 0.05% TFA, and 50 mM HFIP. HFIP was added to the mobile phase to promote ionization efficiency in negative electrospray. The separation was carried out with an initial wash of solvent A for 5 min, 2% gradient of solvent B for 10 min, followed by 1% gradient for 30 min, and a final wash with 90% solvent B for 10 min.

Detection of Aldehyde Products. The Purpald color reaction was performed according to a procedure slightly modified from that in the literature.[57] Purpald was dissolved in 1.0 M NaOH to a concentration of 0.75%; 10 μL of peptide that had been exposed to radiation (a 20-μL sample of 20 μM peptide ARRA irradiated by cesium γ-ray source for 8 min) was mixed with 60 μL of Pupald solution in a 0.2-mL Eppendorf tube, and then 5 μL of 30% H_2O_2 was added to the mixture. The sample was briefly vortexed and allowed to stand for a few minutes, after which the color was noted.

Data Processing. The oxidation products were quantitated according to their peak intensity of mass spectral signals (e.g., no corrections were made for potential ionization efficiency differences between unoxidized and oxidized products) (see Results and Discussion). The amount of unoxidized peptide (fraction unmodified) is calculated by the ratio of peak intensity of unoxidized peptide to the sum of peak intensities of unoxidized peptide and all oxidation products, whereas the amount of a specific oxidation product (fraction modified) was measured by the ratio of its peak intensity to the sum of peak intensities of unoxidized peptide and all oxidation products. The radiolysis of peptides is studied by the dose−response (i.e., the decay of unoxidized peptide or the accumulation of oxidation products as a function of exposure time).

Radiolysis of peptide may generate one or more oxidation products. Such reactions can be expressed by

$$\mathrm{M} \xrightarrow{\text{radiolysis}} \mathrm{P}_1 + \mathrm{P}_2 + \mathrm{P}_3 + \ldots = \sum_{i=1}^{n} \mathrm{P}_i$$

where M stands for the peptide and P_i stands for the oxidation products. We define the initial peptide concentration as 1, M as the fraction of unmodified peptide, and P_i as the fraction of the ith oxidation product. Under the typical footprinting conditions, the peptides are primarily modified at side chains (as opposed to cleavage events[5,8]), thus the total concentration of a specific peptide remains unchanged:

$$\mathrm{M} + \sum_{i=1}^{n} \mathrm{P}_i = 1$$

Radiolysis of water generates hydroxyl radicals. During the exposure time (t), the concentration of radicals rapidly rises to a steady-state level and remains nearly constant during the exposure time.[18] Thus, the initial oxidation reactions of unmodified peptides follow pseudo-first-order kinetics.[12] The decay rate of the unoxidized peptide is

$$\frac{\mathrm{d}\mathrm{M}}{\mathrm{d}t} = -k_{\mathrm{u}}\mathrm{M}$$

where k_u stands for the apparent rate constant and t stands for the reaction time. This equation can be integrated to give

$$M = e^{-k_u t} \quad (1)$$

The apparent rate constant k_u can be obtained by nonlinear fitting of M (fraction unmodified of the peptide) versus t using eq 1.

For the appearance of individual oxidation products, the reactions also follow pseudo-first-order reaction kinetics. The rate of production of the ith oxidation product can be described as follows:

$$\frac{dP_i}{dt} = k_i M$$

where k_i is the rate constant for the formation of product P_i. By substituting eq 1 for M and integrating, we obtain the following eq 2 that defines the fraction of the oxidation product P_i observed at exposure time t:

$$P_i = \frac{k_i}{k_u}(1 - e^{-k_u t}) \quad (2)$$

The use of fraction oxidation product is key to analyzing the products using mass spectrometry, where the inconsistency of ionization efficiency from experiment to experiment necessitates the use of a ratio method for the quantitation. However, the drawback of this approach is that the apparent rate is influenced by the relative ionization efficiency of the unmodified peptide relative to the ionization products. This is an important subject of the paper emphasized in the Results and Discussion. However, as a result, the observed rate constants must be interpreted semiquantitatively. Future experiments are underway to probe the relative ionization efficiencies of the various modification products relative to the unmodified peptide. Nevertheless, the rate constant for the formation of individual oxidation product (k_i) is obtained by nonlinear regression of P_i (fraction modified oxidation product) versus exposure time (t). With this approach, the sum of the rate constants of all oxidation products is equal to the apparent rate constant for the disappearance of the peptide:

$$\sum_{i=1}^{n} k_i = k_u \quad (3)$$

RESULTS AND DISCUSSION

Radiolytic Oxidation Mechanism of Arginine. Arginine is expected to be quite susceptible to attack by hydroxyl radicals.[50−56] The oxidation may lead to the cleavage of the guanidino group and conversion of arginine to a γ-glutamyl semialdehyde residue. As the most basic amino acid residue with pK_a ~12.5, arginine typically carries a positive charge and arginine-containing peptides provide a strong signal when positive ion ESI-MS is employed. Destruction of arginine will significantly reduce the ionization efficiency of Arg-containing peptides in positive ion ESI-MS, while it is not expected to influence the efficiency of ESI in negative ion mode. Therefore, a model peptide containing two arginine residues, Ala-Arg-Arg-Ala, and another peptide containing only one arginine residue, Asp-Ser-Asp-Pro-Arg (see below), were selected for radiolytic oxidation and analysis.

The peptides were exposed to synchrotron X-rays and cesium-137 γ-rays. The positive ESI-MS spectrum of ARRA irradiated by γ-rays for 4 min is shown in Figure 1A. The peak at m/z 473.3 belongs to the molecular ion of the unmodified peptide. The major modified product has the second most intense signal at m/z 430.3 Da, which is 43 mass units lower than that of the unmodified peptide. Other oxidation products include those with m/z values of 400.2, 416.2, 443.3, 462.2, 487.2, and 489.2.

Tandem mass spectra were acquired to determine the modification sites on the peptide for each oxidation product using collision induced dissociation (CID). The Biemann nomenclature system was used for naming the peptide fragment.[58] Cleavage of the peptide chain in the collision cell can occur at the $C_\alpha-C$, C−N, or $N-C_\alpha$ bonds within the peptide, and these cleavage events yield six types of fragments that are labeled a_n, b_n, and c_n, when a positive charge is retained on the N-terminal side of the peptide; and x_n, y_n, and z_n, when a positive charge is retained on the C-terminal side, with the n value denoting the size of the fragment in amino acids. The MS/MS spectrum of ion m/z 430.3 (−43 Da) (Figure 1B) revealed that the 43 Da mass loss is from either of the two arginine residues. The peak at m/z 341.1 is the b_3-43 CID ion, while the peak at m/z 359.2 corresponds to the y_3-43 ion. No b_3 and y_3 were found. The presence of b_3-43 and y_3-43 and the absence of b_3 and y_3 ions indicate unambiguously that either of the two arginine residues were oxidized and exclusively responsible for the mass change of −43 Da. The peak at m/z 228.1 is the unmodified b_2 ion, while the weak peak at m/z 246.1 is the unmodified y_2 ion. The presence of b_2 and y_2 ions indicates that both arginine residues experience the 43 Da mass loss. A weak b_2-43 is also found at m/z 185.1. Because the charge is retained at the unmodified arginine residue, the low-energy collision gives no observed signal for y_2-43 and only a very weak signal for b_2-43 ions.

The oxidation of arginine by metal ion-catalyzed oxidation (MCO) systems has been reported.[50−56] Amici et al.[50] treated polyarginine with Fe(II)/EDTA/O_2. The oxidized homopolymers were reduced with $NaBH_4$, hydrolyzed with 6 N HCl, and analyzed using an amino acid analyzer. The reduction product of oxidized arginine was identified as 5-hydroxy-2-aminovaleric acid. Later, the production of γ-glutamyl semialdehyde in amino acid homopolymers and proteins oxidized by MCO systems was confirmed by amino acid analysis and GC/MS; its reduced species, 5-hydroxyl-2-amino valeric acid, has been used as specific marker of oxidized arginine in proteins.[51−56]

The mechanism of arginine oxidation for the formation of the −43 Da product, as presented in the literature for metal-catalyzed oxidation, is presented in Scheme 1.[50,52] A hydroxyl radical abstracts a hydrogen from the δ-carbon of the side chain and adds a hydroxyl group to form an intermediate oxidation product with +16 Da mass as compared to the parent arginine residue; the subsequent loss of the guanidino group from the +16 Da precursor oxidation product leads to γ-glutamyl semialdehyde. A similar oxidation of arginine is expected to take place under

(57) Dickinson, R. G.; Jacobsen, N. W. *Chem. Commun.* **1970**, 1719−20.

(58) Biemann, K. *Methods Enzymol.* **1990**, 886−7.

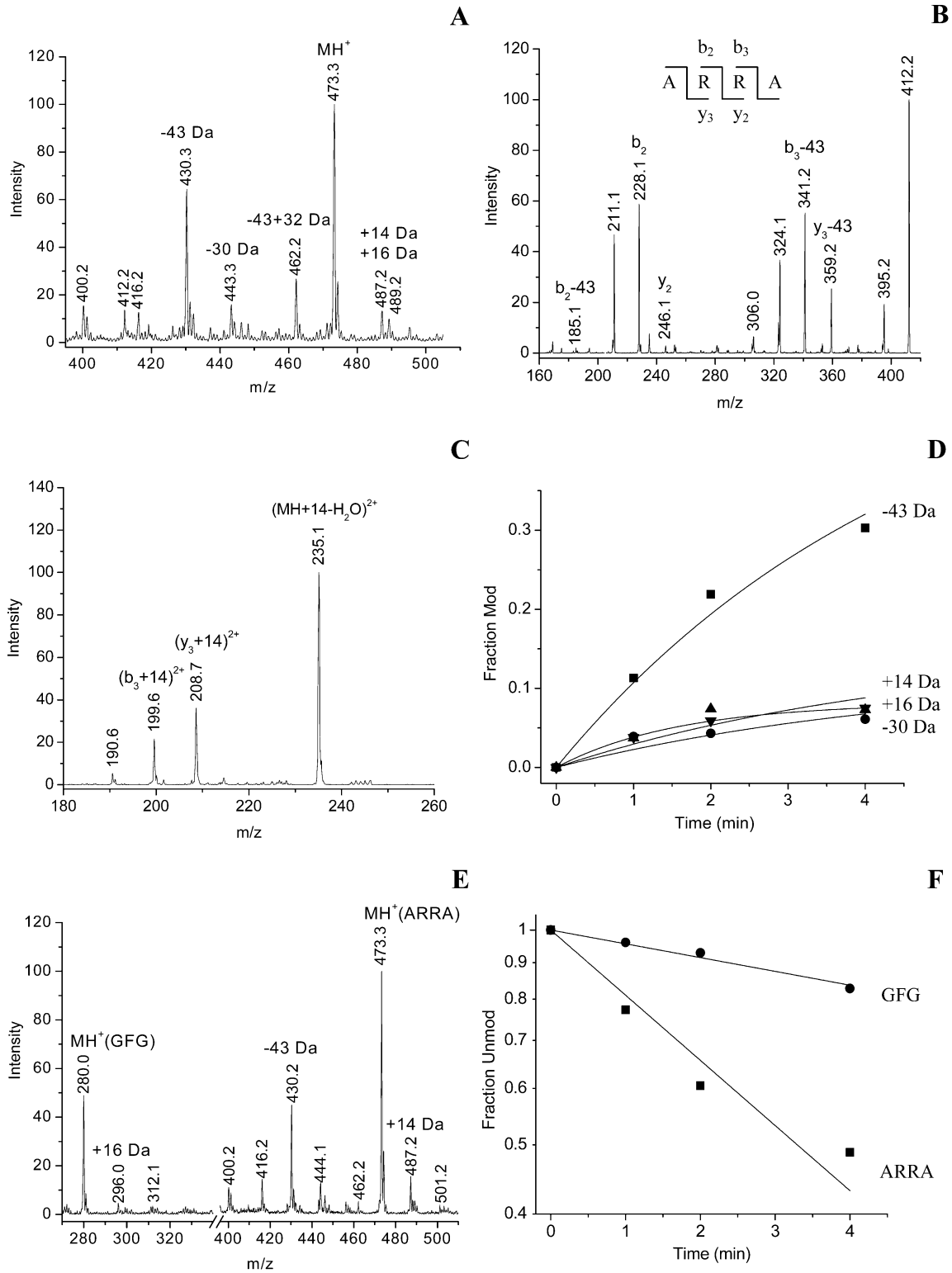

Figure 1. Mass spectral data of peptides ARRA and GFG. The exposed samples were diluted to 10 μM using CH_3OH or acetonitrile (only for synchrotron exposed mixed peptides in panel E), and analyzed by ESI-MS without chromatographic separation. (A) Positive ion ESI mass spectrum of ARRA exposed to cesium-source γ-rays for 4 min. (B) MS/MS spectrum of ion at *m*/*z* 430 (−43 Da) of ARRA. (C) MS/MS spectrum of ion at *m*/*z* 244 [$(MH_2 + 14)^{2+}$] of ARRA. (D) Dose−response of oxidation products of ARRA exposed to γ-rays based on negative ESI-MS. (E) Positive ion ESI mass spectrum of 20 μM ARRA and 20 μM GFG mixture exposed to synchrotron X-rays for 15 ms. (F). Dose−response of ARRA and GFG irradiated by γ-rays. The solid lines are fits to the data as described in the Experimental Procedures section.

radiolytic conditions. To provide support for this mechanism under radiolytic conditions, we tested for the presence of an aldehyde group after arginine oxidation by use of a color reaction. Purpald (4-amino-3-hydrazino-5-mercapto-1,2,4-triazole) is an exceedingly specific and sensitive reagent for testing aldehyde.[57] Even though Purpalde reacts with both aldehydes and ketones, only the aldehyde product is further oxidized to yield a purple-to-magenta-colored aromatic heterocyclic product (6-mercapto-s-triazolo-

Scheme 1. Proposed Mechanism for Formation of −43 Da Oxidation Product from Arginine Residue

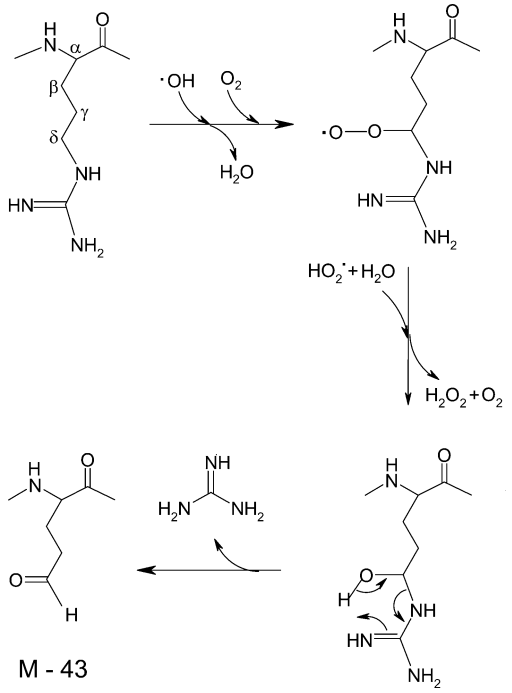

[4,3b]-*s*-tetrazines) on exposure to air or hydrogen peroxide. Esters and amides will not react with Purpald. The color reaction was carried out on γ-ray-exposed ARRA peptide as outlined in the Experimental Procedures section; a magenta product was formed after a few minutes. The characteristic color change unambiguously supports that aldehyde was formed by oxidation of arginine, as shown in Scheme 1.

The MS/MS of ion m/z 462.2 (not shown) was examined to investigate its identity. The ion fragmented to produce a series of weak signals identical to those in the MS/MS spectrum of ion m/z 430.3 (Figure 1B) and a very intense major fragment ion at m/z 430.3, whose CID spectrum (e.g., the MS/MS/MS spectrum of the fragment ion from ion m/z 462.2) was identical to that of the MS/MS spectrum of ion m/z 430.3 (Figure 1B). When acetonitrile instead of methanol was added to the samples as the spray solvent (as in the case of Figure 1E), the ion signal at m/z 462.2 was greatly reduced. The mass difference between these two peaks m/z 430.3 and 462.2 is 32 Da, which is the molecular weight of methanol. Therefore, we believe that the m/z 462.2 ion was the hemiacetal (−43 + 32 Da) generated from the species at m/z 430.3 by reaction with methanol. The formation of hemiacetal also supports that the −43 Da product was an aldehyde as shown in Scheme 1.

The peaks at m/z 487.2 and 489.3 were oxidation products with +14 and +16 Da mass additions, respectively. The +14 and +16 Da species also appeared as doubly charged ion signals at m/z 244 and 245, respectively. The MS/MS spectrum of the doubly charged ion of +14 species at m/z 244 ion is presented in Figure 1C. The peak at m/z 235.1 apparently results from the loss of water from the parent ion. The peaks at m/z 199.6 and 208.7 were the $(b_3+14)^{2+}$ and $(y_3+14)^{2+}$ fragments, respectively. No b_3^{2+} and y_3^{2+} or b_3 and y_3 fragments were found. This result indicates that +14 Da was *exclusively* located on the two arginine residues. The MS/MS spectrum of the double-charged +16 Da species (not shown) at m/z 245 was similar to that of +14 Da species at m/z 244. The $(b_3+16)^{2+}$ and $(y_3+16)^{2+}$ fragments were found at m/z 200.7 and 209.7, respectively, and no b_3^{2+} and y_3^{2+} or b_3 and y_3 fragments were found. The data indicate that the two arginine residues were also responsible for the +16 Da products.

The radiation-exposed peptide ARRA samples were also analyzed by negative ion ESI-MS (data not shown). The negative mass spectra were similar to those positive spectra. The −43 Da product appeared as a singly charged ion in both positive and negative ESI-MS. However, the unmodified peptide and the +14 and +16 Da products clearly appeared as both singly and doubly charged ions in positive ESI-MS but only as singly charged ions in negative ESI-MS. A very weak peak corresponding to loss of both guanidino groups (−43 × 2 Da) was found in negative spectrum but not in the positive spectrum as result of decreased ionization efficiency in positive ion electrospray.

Elimination of CO_2 in the Radiolytic Oxidation of Peptides. The peak at m/z 443.3 is 30 mass units lower than that of unmodified peptide. MS/MS data (not shown) indicate the 30 Da mass loss was exclusively located at the C-terminal alanine residue. We have also observed this behavior in other peptides (data not shown). At the C-terminus (as is the case for glycine and alanine internally), due to reduced steric hindrance, the α-carbon hydrogen can be readily abstracted and an alkoxyl radical is formed at the C-terminal α-carbon. The decomposition of the alkoxyl radical results in C-terminal decarboxylation and formation of a C-terminal aldehyde for glycine and ketone for other amino acid residues and can explain the −30 Da mass change.[59] The peak m/z 400.2 was likely due to oxidative decarboxylation of C-terminal alanine plus loss of the guanidino group, while the peak m/z 416.2 was likely caused by additional oxidation of species m/z 400.2.

Reactivity of Arginine under Radiolysis Conditions. The individual oxidation products of ARRA were accumulated exponentially as a function of exposure time. The relative amounts of the unoxidized peptide and oxidation products were estimated from the intensity of negative ion ESI mass spectral signals. The amounts of the different oxidation products were calculated as described in Experimental Procedures. The dose−response curve for the four major oxidation products (−43, +14, +16, and −30 Da) are presented in Figure 1D. The rate constants of formation of different products were obtained by nonlinear regression of the fraction unmodified verse exposure time (t) as described in the Experimental Procedures and are listed in Table 2. The rate constants for the production of −43, +14, +16, and −30 Da are 0.119, 0.033, 0.031, and 0.025 min^{-1}, respectively. The primary oxidation product was the species with 43 Da mass reduction, which was formed ∼3−4 times faster than +14 and +16 Da products.

The faster rate of production of the −43 Da product is consistent with a preferred initial abstraction of hydrogen from the δ-carbon of arginine as initial β- or γ-abstraction events can lead only to +14 or +16 products. This preference for the δ-carbon has been identified by deuterium exchange NMR studies[60] and by EPR spin trapping studies.[61] Under anaerobic conditions,[60] when amino acids in D_2O buffer were irradiated by γ-rays,

(59) Davies, M. J. *Arch. Biochem. Biophys.* **1996**, *336* (1), 163−72.
(60) Nukuma, B. N.; Goshe, M. B.; Anderson, V. E. *J. Am. Chem. Soc.* **2001**, *123*, 1208−14.

Table 2. Rate Constants for Modifications of Peptides Irradiated by Cesium-137 γ-rays or Synchrotron X-rays

ARRA exposed to γ-ray		GFG exposed to γ-ray	
+14 Da	0.033 ± 0.004 min^{-1}	peptide	0.044 ± 0.009 min^{-1}
+16 Da	0.031 ± 0.004 min^{-1}		
−43 Da	0.119 ± 0.004 min^{-1}		
−30 Da	0.025 ± 0.004 min^{-1}		
peptide	0.210 ± 0.015 min^{-1}		

DSDPR exposed to γ-ray		DAHK exposed to synchrotron X-ray	
−30 Da	0.011 ± 0.001 min^{-1}	His −22 & −40 Da	12.2 ± 0.2 s^{-1}
−43 Da	0.020 ± 0.001 min^{-1}	His +16 Da	1.5 ± 0.2 s^{-1}
+14 Da	0.032 ± 0.001 min^{-1}	His −10 Da	4.7 ± 0.2 s^{-1}
+16 Da	0.030 ± 0.001 min^{-1}	His +5 Da	6.4 ± 0.2 s^{-1}
peptide	0.094 ± 0.004 min^{-1}	Lys +14 & +16 Da	10.4 ± 0.2 s^{-1}
		peptide	35.2 ± 0.3 s^{-1}

hydroxyl radical abstraction produced carbon-center amino acid radicals, which exchanged ^{2}H from D_2O. The relative propensity of •OH-promoted ^{1}H/^{2}H exchange represents the relative sensitivity to hydroxyl radical attack. For L-arginine, ^{2}H was incorporated into all methylene side-chain carbons with a ratio of 11:3:1 for δ-CH_2, γ-CH_2, β-CH_2, respectively (e.g., oxidation at the δ-position was preferred 70−75% of the time). EPR was used to investigate the reaction of hydroxyl radicals generated by UV photolysis of H_2O_2 with 14 aliphatic amines, polyamines, and compounds containing one and two guanidino groups.[61] For the amines and polyamines below pH 7, the predominant reaction of hydroxyl radical was the abstraction of hydrogen atom from the carbons not adjacent to the protonated amino group. In contrast, for the two compounds containing one and two guanidino groups, the hydrogen abstraction occurred at the carbon adjacent to guanidino groups. This indicates that the C−H bonds vicinal to the guanidino group are particularly susceptible to hydrogen-atom abstraction by hydroxyl radicals. The data in this study indicate that the −43 Da product is formed ∼65% of the time, very close to the NMR predicted value. This implies that almost all of the δ-carbon abstractions lead to the −43 Da product (e.g., the +16 Da product initially formed after abstraction of hydrogen at the δ-carbon is not stable). This is reasonable since the pseudoaromatic electron-delocalized guanidino π-system provides an electron sink promoting the formation of the aldehyde product. It follows that the +14 and 16 Da products observed arise from initial abstraction at the γ- and β-positions.

The reactivity of arginine was compared with phenylalanine by mixing two separate peptides and comparing their oxidation rates. A solution containing both 40 μM ARRA and 40 μM GFG was exposed to the synchrotron X-ray beam for 15 ms. The irradiated sample was diluted to 10 μM using acetonitrile before analysis by mass spectroscopy. The positive mass spectrum is shown in Figure 1E. The peak m/z 280.0 was the unmodified peptide GFG, while the weak peaks at m/z 296.0 and 312.1 were its oxidation products. The signals between m/z 400 and 510 were from oxidized ARRA as previously described. The signals of oxidation products of ARRA were much more intense than those of GFG, indicating that the two arginine residues in ARRA competed effectively for hydroxyl radicals with the phenylalanine contained in the GFG peptide.

Radiolysis by synchrotron X-ray and low-flux γ-ray sources produced similar oxidation products except on different time scales. On the basis of the comparison of Figure 1, panels A and E, the exposure to the low-flux γ-rays for 4 min produced levels of oxidation slightly less than seen for synchrotron X-ray exposure for 15 ms. Because the two peptides were oxidized too rapidly by synchrotron X-rays to give an accurate dose−response (the shutter's lower limit is 7 ms), the dose−response was performed using the cesium γ-ray source. The fraction of unmodified peptides was calculated by the ratio of peak intensity of the unmodified peptide to the sum of peak intensity of both unmodified peptide and all modified products. The fraction of unmodified peptides as a function of exposure times was fitted as described in the Experimental Procedures and is shown in Figure 1F. The rate constant for the loss of ARRA was 0.210 min^{-1}, which was about 5 times that of GFG, at 0.044 min^{-1} (Table 2). Taking into account that there are two arginine residues in ARRA, this gives a rate for that peptide of 0.105 arginine^{-1} min^{-1}, more than two times that observed for phenylalanine. Table 1 indicates that the rate of initial reaction of hydroxyl radicals with phenylalanine is faster than the initial reaction with arginine. However, the results here clearly indicate that the stable oxidation products for arginine in ARRA accumulate more rapidly.

To determine the sequence specificity of arginine oxidation to −43 Da products, we examined radiolysis of other arginine-containing peptides. The peptides included KRSR, TRKR, RPPGFSPFR, GRADSPK, RVDSADESNDDGFD, RGVVNASSRLAK, RREEETEEE, and KKRAARARATS-NH_2. These peptides were dissolved in water at a concentration of 20 μM, exposed to γ-rays for 6 min. Because all of these peptides except RVDSADESNDDGFD contained one or more additional basic amino acid residuals in addition to the arginine, the −43 Da products were observed in both positive and negative ESI mass spectra. Compared to the prevalence of +16 and +14 Da products, the signal corresponding to −43 Da is much stronger in KRSR, TRKR, and RREEETEEE; relatively weaker in KKRAARARATS-NH_2 and RGVVNASSRLAK; much weaker in RPPGFSPFR and GRADSPK; and absent in RVDSADESNDDGFD. Thus, the reactivity of individual arginine residues and/or the relative ionization efficiency of the modified products is strikingly sequence- and structure-dependent. We are currently exploring the chemical basis of these differences. However, this fact and the lack of a precise estimate of the ionization efficiency of the modified Arg products suggest that absolute conclusions about the reactivity of Arg must be cautiously drawn.

Arginine Oxidation in DSDPR. We also examined the radiolytic oxidation of Asp-Ser-Asp-Pro-Arg (DSDPR), a peptide containing only one arginine residue. The positive and negative ion electrospray mass spectra of peptide DSDPR irradiated by the cesium-137 γ-ray source for 4 min are shown in Figure 2A,B. The ion at m/z of 589.3 in the positive mass spectrum and the ion at m/z 587.2 in the negative mass spectrum belong to the unmodified peptide. The oxidation product with a 43 Da mass reduction was observed at m/z 544.1 in the negative ion spectrum; no corresponding signal was found in the positive ion spectrum. The MS/MS spectrum of the negative ion m/z 544.1 (not shown) indicates

(61) Mossoba, M. M.; Rosenthal, I.; Riesz, P. *Can. J. Chem.* **1982**, *60*, 1493−500.

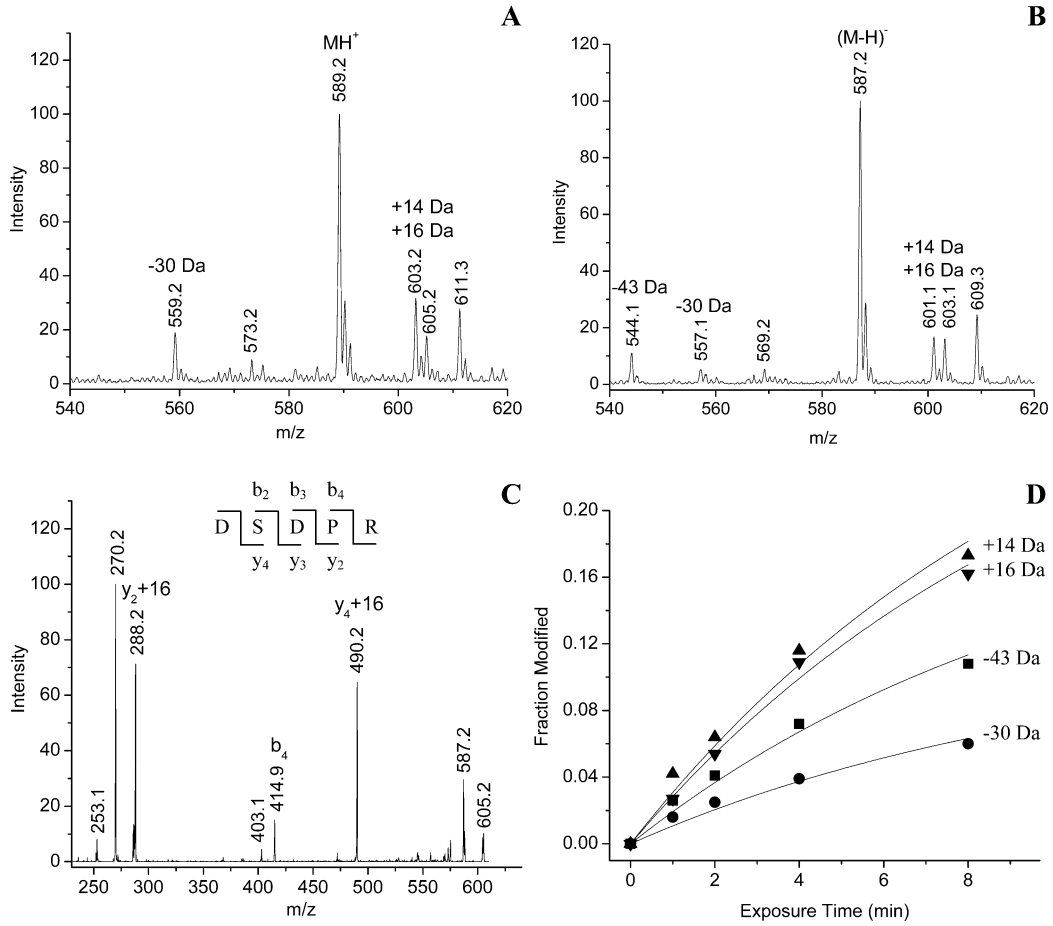

Figure 2. Mass spectral data of peptide DSDPR. (A) Positive and (B) negative ion ESI mass spectra of DSDPR exposed with the cesium-source γ-rays for 4 min. (C) MS/MS spectrum of ion *m*/*z* 605 (+16 Da). (D) Dose−response of various oxidation products. The solid lines are fits to the data as described in the Experimental Procedures section.

that the 43 Da mass loss is from arginine. Apparently, the destruction of the charged arginine residue significantly decreased the ionization efficiency of the peptide in positive ion ESI-MS, which relies on the basic residue to carry positive charge for efficient ionization. However, the destruction of arginine did not similarly affect the ionization efficiency in negative electrospray experiments, which relies on the acidic amino acid residues and the C-terminal carboxyl group to carry negative charges for efficient ionization.

The positive ions at m/z 603.2 and 605.2 were the oxidation products exhibiting +14 and +16 Da mass additions. The MS/MS spectrum of the ion with m/z 605.2 (Figure 2C) indicates that the C-terminal arginine is responsible for the +16 Da oxidation product. The spectrum gave a very strong y_2+16 signal at m/z 288.2 and y_4+16 signal at 490.2 but no y_2 and y_4 signals, indicating that +16 Da addition was located at Pro or Arg. The presence of intense b_4 ion at m/z 414.9 and the absence of b_4+16 ion further indicate that the oxidative +16 mass addition was exclusively or at least mostly occurred at the C-terminal arginine. As for the +14 Da oxidation product, the MS/MS spectrum of positive ion m/z 603.2 (not shown) indicates that both arginine and proline are responsible for the +14 Da mass addition.

The mass reduction of 30 Da seen in Figure 2A,B results from oxidative decarboxylation (as seen above) of C-terminal Arg and the two Asp residues in the peptide DSDPR. The species showed a signal at m/z 559.2 in the positive spectrum and a weaker signal at m/z 557.1 in the negative spectrum. The MS/MS spectra of positive and negative ions of the oxidized product provided complementary information for determining the sites of oxidation and indicated that both Asp residues and the C-terminal Arg residue were responsible for the 30 Da mass reduction (e.g., they were all susceptible to oxidative decarboxylation by radiolysis). The oxidation of acidic amino acid residues and their application to protein footprinting will be the subject of a future publication.

The dose−response curves of different oxidation products for peptide DSDPR irradiated by cesium-137 source γ-rays based on the negative electrospray mass spectra are shown in Figure 2D. The rate constants are presented in Table 2 and are 0.011, 0.020, 0.032, and 0.030 min^{-1} for the −30, −43, +14, and +16 Da oxidation products, respectively. As demonstrated in Figure 2A,B, the −30 Da C-terminal oxidative decarboxylation product was under-represented in negative mass spectra, because the loss of C-terminal carboxylic acid decreased its ionization efficiency in negative electrospray. For arginine, since it was located at C-terminus, oxidative decarboxylation competed with the oxidation of the side chain and thus decreased the apparent rate of formation of the −43 Da oxidation product. However, the data of Table 2 indicate that arginine is oxidized up to five times more efficiently than proline within this specific sequence as it accounts for all of the observed −43 Da and +16 Da products and for roughly half of the +14 Da oxidation products.

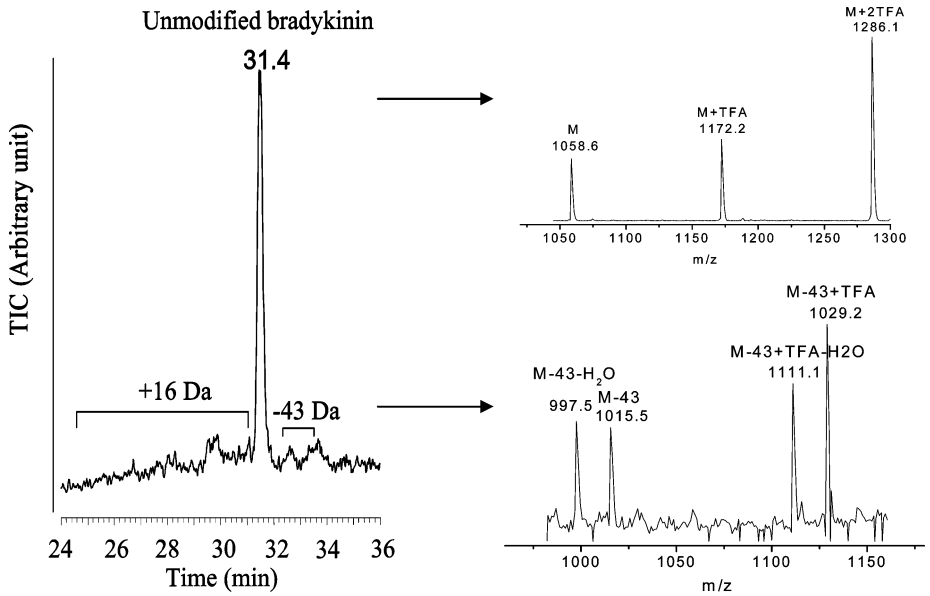

Figure 3. Negative ion HPLC-MS of arginine oxidation products. The total ion chromatogram of bradykinin exposed to γ-rays for 5 min is shown in the left-hand panel. The MS spectrum in the upper right is that of unmodified bradykinin seen at 31.4 min. The unmodified ion and the ion bound to one or two TFA adducts is shown. The lower right-hand panel shows the −43 Da oxidation product of bradykinin seen at 32−34 min.

The above mass spectral data clearly explain why the oxidation of arginine has not been observed previously in hydroxyl radical mediated protein footprinting experiments. For many sequences, the oxidation of arginine builds up a primary product as a function of dose at mass −43 Da instead of the +16 Da or +14 Da mass changes observed for most other amino acid residues.[12] At the same time, protein digests are generally separated by HPLC in low pH and analyzed by ESI-MS in positive ion mode. The destruction of arginine dramatically decreases the ionization efficiency of the −43 Da species versus the unmodified peptides in the positive electrospray, and thus the −43 Da species is silent. An additional complication is obvious when we consider the overall protein footprinting approach when trypsin is used to generate the protein digest. Once the guanidino group is eliminated, trypsin is no longer able to recognize the cleavage site. Use of other proteases circumvents this disadvantage[5,6,28] and will likely allow oxidized arginine to be easily detected in future experiments.

HPLC Negative-ESI-MS Analysis of Arginine-Contained Peptides. Although the −43 Da oxidation products can be observed using MALDI-MS in negative mode, HPLC-ESI-MS is preferred for its superior resolving power and superior potential for quantitative analysis. As discussed above, for peptides without basic amino acid residues in addition to arginine, the −43 Da product is observable only using negative ESI-MS. For those peptides containing one or more basic amino acid residues in addition to the target arginine, even though the −43 Da product is still observable by ESI-MS in positive mode, the −43 Da products were more easily detected by negative ESI. Our ordinary separation methods using reverse-phase HPLC under acidic conditions (around pH 2 with addition of TFA or formic acid), suffer from poor ionization efficiency in negative electrospray. The addition of hexafluoro-2-propanol to the mobile phases promotes the ionization efficiency of negative electrospray without negatively impacting separation.

HPLC negative-ESI-MS was used for analysis of the oxidation products of the arginine containing peptide bradykinin. Figure 3 shows the total ion current chromatogram of bradykinin exposed to γ-rays for 5 min and the corresponding negative electrospray signals of the unmodified and −43 Da oxidation product. TFA adducts were also formed in negative ESI-MS. The intense peak at a retention time of 31.4 min is unoxidized bradykinin. The peaks observed between 32 and 34 min correspond to −43 Da oxidation products; the loss of the guanidino group reduces the polarity, thus increasing the retention time relative to the unoxidized peptide. The separate oxidation of arginine residues at the C- and N-terminus of bradykinin results in the two distinct species with different retention times. The broad bands between 24 and 31 min are due to +16 and +14 Da oxidation products. The oxygen additions occur at different sites on the peptides generating products with various retention times; the oxygen addition also results in a more polar product with a decreased retention relative to the unoxidized species. These data indicate that HPLC-ESI-MS of oxidized arginine peptides is feasible and illustrate a specific method for analyzing protein digests in footprinting experiments.

Radiolytic Oxidation of Histidine and Lysine. The peptide DAHK was exposed to synchrotron X-rays for 10−25 ms. The mass spectrum of the peptide irradiated for 25 ms is shown in Figure 4A. The peak at m/z 470.2 belongs to the unmodified peptide. The modified products included m/z 430.1, 448.1, 460.2, 475.2, 484.2, and 486.1. The peak at m/z 430.1 was likely due to loss of a water molecule from the species m/z 448.1. Excluding the peak at m/z 430.1, we observed five oxidation products for this peptide as a function of exposure time. The MS/MS spectrum of the ion at m/z 448.1 (mass reduction of 22 Da) is shown in Figure 4B. The fragments m/z 262.1 and 333.1 belonged to y_2-22 and y_3-22. No y_2 and y_3 fragments were found. The presence of y_2-22 and y_3-22 and the absence of y_2 and y_3 fragments indicate that the −22 Da mass loss is located at His or Lys. The fragments m/z 186.9 and 302.0 were b_2 and b_3-22, respectively. No b_2-22 and b_3 fragments were found. The data indicate that the −22 Da mass loss is attributable to His. Apparently, the ion m/z 448.1 corresponds to the oxidation product in which the

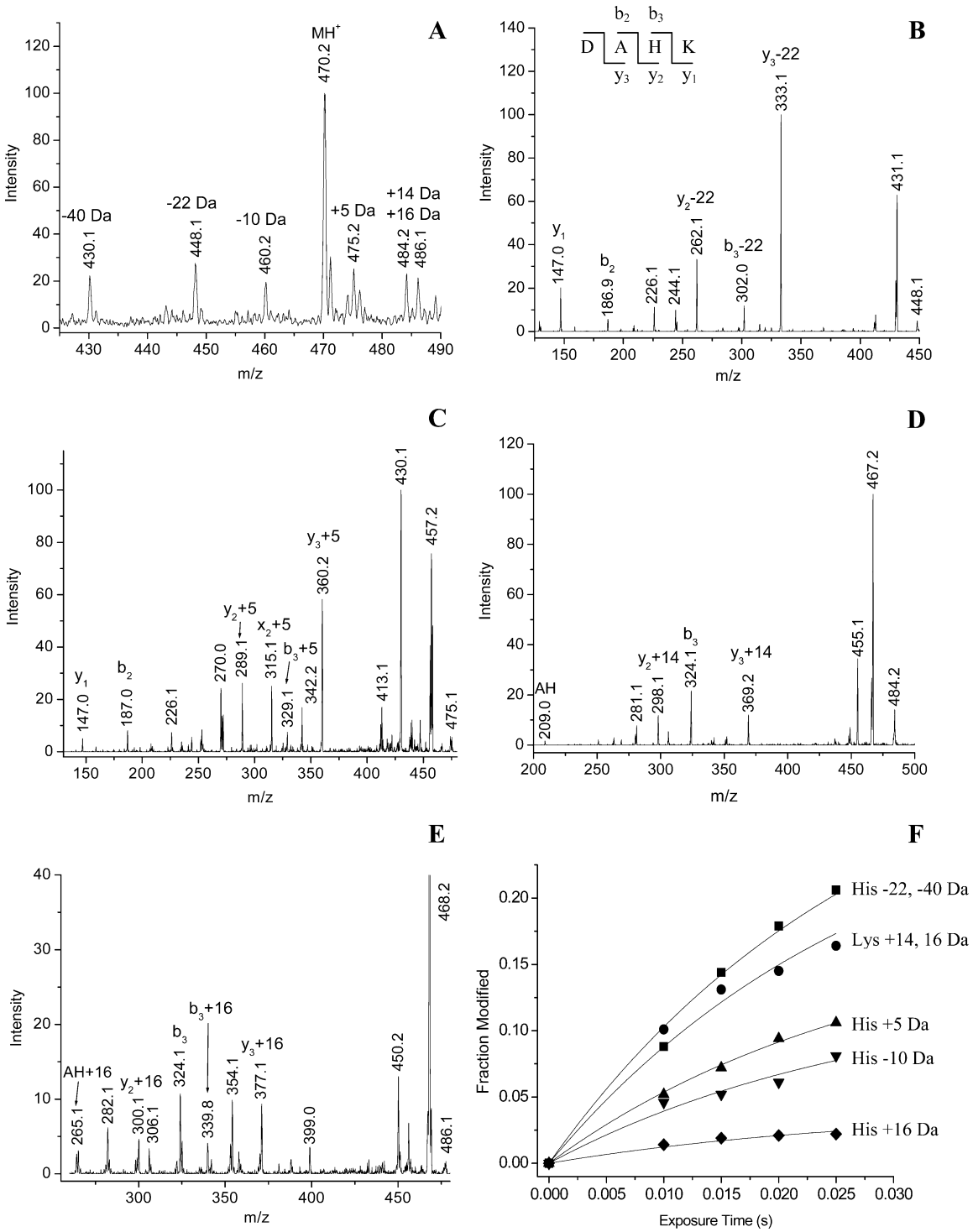

Figure 4. Mass spectral data of peptide DAHK irradiated by synchrotron X-rays. (A) Positive mass spectrum of DAHK exposed for 25 ms. (B) MS/MS spectrum of ion at *m*/*z* 448 (−22 Da). (C) MS/MS spectrum of ion at *m*/*z* 475 (+5 Da). (D) MS/MS spectrum of ion at *m*/*z* 484 (+14 Da). (E) MS/MS spectrum of ion *m*/*z* 486 (+16 Da). (F) Dose response of various oxidation products. The solid lines are fits to the data as described in the Experimental Procedures section.

histidine residue had been converted to aspartic acid, consistent with MCO studies of histidine oxidation[35] (see Scheme 2 and below).

The peak *m*/*z* 475.2 corresponded to the product with a mass addition of 5 Da over the original peptide. The MS/MS spectrum of ion *m*/*z* 475.2 is shown in Figure 4C. The peaks *m*/*z* 289.1 and 360.2 belonged to y_2+5 and y_3+5. No y_2 and y_3 signals were found. The presence of y_2+5 and y_3+5 and the absence of y_2 and y_3 fragments indicate that the +5 Da mass loss was located at His or Lys. The signals *m*/*z* 187.0 and 329.1 were b_2 and b_3+5 fragments, respectively. No b_2+5 or b_3 fragments were found. Thus, the +5 Da mass addition is located at His. This product was possibly formyl-asparigine with the structure shown in Scheme 2. It was previously identified as a product of histidine oxidation in the study of *N*-benzoylhistine oxidized by the Cu^{2+}/H_2O_2 system.[62] The peak at *m*/*z* 460.2 corresponded to the

Scheme 2. Primary Oxidation Products of Histidine

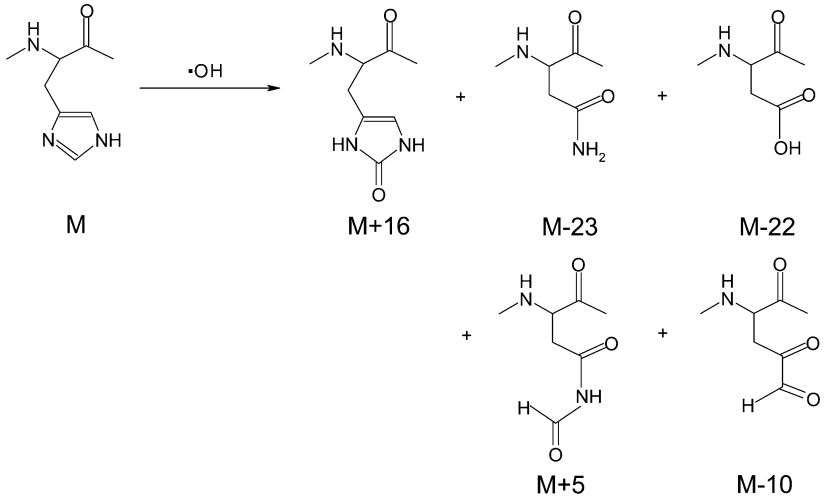

products with a mass reduction of 10 Da relative to the original peptide. The MS/MS spectrum of m/z 460.2 (not shown) also indicates that the 10 Da mass reduction is located on the histidine residue. This product of histidine has not been reported before. Based on the change of molecular weight, the M−10 Da product could have the structure as shown in Scheme 2.

The reaction of histidine with hydroxyl radicals is complicated, and all the oxidation products have not been fully characterized.[32,33] The complexity of histidine oxidation has been demonstrated by metal ion-catalyzed oxidation. Hydroxyl radicals initially attack the imidazole ring of histidine at positions C-2, C-4, and C-5 and produce the stabilized allyl-type radicals.[63−66] These radicals can incorporate O_2 to give peroxyl radicals and undergo further reactions giving rise to a mixture of products that depend on the reaction conditions and the local amino acid sequences.[62,67−71] 2-Oxohistidine, asparagines, and aspartic acid have been identified as the major products. Uchida and Kawakishi[62] investigated the damage of histidine within proteins using Cu_2^+/H_2O_2 and *N*-benzoylhistidine as the model compound. Four products including asparagines, aspartic acid, aspartylurea, and formyl-asparagine were observed, emphasizing the rupture of imidazol ring. Even more complex reactions were indicated in the case of photooxidation. Tomita et al.[72] demonstrated that histidine was photooxidized to aspartic acid via several intermediate compounds. In addition to the final product, they detected and isolated 17 intermediate products of the reaction.

The radiolytic oxidation of histidine residues is also expected to be complex and dependent upon both the reaction conditions and the molecular environment in proteins (i.e., both sequence and structure). For example, pH is expected to play an important role in the oxidation. At a pH below pK_a ~6.0, histidine carries a positive charge, which tends to deactivate the residue by decreasing its electron density. The radiolytic products of histidine could be similar to those produced by MCO systems. Dean et al.[70] demonstrated that histidine residues in a protein was substantially converted into aspartic acid by exposure to hydroxyl radicals generated by Cu^{2+}/H_2O_2 or by γ-radiolysis. The major oxidation products of His residues as proposed here and in the literature are presented in Scheme 2.[62,70] The complex mechanism of the histidine oxidation as well as its response to sequence and reaction conditions requires further investigation; however, the data above provide valuable insight as to where to look for oxidized products to maximize the value of histidine as a footprinting probe.

Lysine was reported to be converted to hydroxylysine[73] and α-aminoadipylsemialdehyde[74,75] by oxidation with MCO or γ-radiolysis.[76] In the presence of oxygen, hydroxyl radicals may abstract hydrogen from and add a hydroxyl group to any carbon of the lysine side chain to give different hydroxylysine products. If hydroxyl attacks the ϵ-carbon, ϵ-hydroxylysine is formed. However, ϵ-hydroxylysine is not stable and becomes 2-aminoadipylsemialdehyde by loss of an ammonia.[75]

The mass spectral and tandem mass spectral data indicate that the lysine residue in the DAHK peptide experienced oxidation. The oxidation of lysine led to products with mass addition of 14 Da, corresponding to the ions m/z 484.2 in Figure 4A. The MS/MS spectrum of ion m/z 484.2 (+14 Da product) is shown in Figure 4D. The presence of intense fragments y_2+14 at m/z 298.1 and y_3+14 at m/z 369.2 and the absence of y_2 and y_3 indicate that the last two amino acid residues H or K were responsible for the +14 mass addition. Furthermore, the presence of b_3 at m/z 324.1 and internal fragment AH at m/z 209.0 from the intact peptide and the absence of b_3+14 unambiguously identify that the +14 Da mass addition was located at the C-terminal lysine. The +14 Da mass addition indicates the formation of a carbonyl in the side

(62) Uchida, K.; Kawakishi, S. *J. Agric. Food Chem.* **1990**, *38*, 660−4.
(63) Rao, P. S.; Simic, M.; Hayon, E. *J. Phys. Chem.* **1975**, *79* (13), 1260−3.
(64) Samuni, A., Neta, P. *J. Phys. Chem.* **1973**, *77*, 1629−35.
(65) Tamba, M.; Torreggiani, A. *Int. J. Radiat. Biol.* **1998**, *74* (3), 333−40.
(66) Lassmann, G.; et al. *J. Phys. Chem. A* **1999**, *103*, 1283−90.
(67) Stadtman, E. R. *Free Radical Biol. Med.* **1990**, *9* (4), 315−25.
(68) Schoneich, C. *J. Pharm. Biomed. Anal.* **2000**, *21* (6), 1093−7.
(69) Uchida, K.; Kawakishi, S. *FEBS Lett.* **1993**, *332* (3), 208−10.
(70) Dean, R. T.; Wolff, S. P.; McElligott, M. A. *Free Radical Res. Commun.* **1989**, *7* (2), 97−103.
(71) Kopoldova, J.; Hrncir, S. *Z. Naturforsch.* [*C*] **1977**, *32* (7−8), 482−7.
(72) Tomita, M.; Irie, M.; Ukita, T. *Biochemistry* **1969**, ***8*** (12), 5149−60.
(73) Trelstad, R. L.; Lawley, K. R.; Holmes, L. B. *Nature* **1981**, *289* (5795), 310−2.
(74) Diedrich, D.; Schenaitman, L. *Proc. Natl. Acad. Sci. U.S.A.* **1978**, *75* (8), 3708−12.
(75) Requena, J. R.; Stadtman, E. R. *Biochem. Biophys. Res. Commun.* **1999**, *264*, 207−11.
(76) Morin, B.; et al. *Chem. Res. Toxicol.* **1998**, *11*, 1265−73.

chain of Lys. However, the carbonyl product was not the 2-aminoadipylsemialdehyde as reported in the literature[50,67,73] because the lysine aldehyde should have a mass reduction of 1 Da as compared to the original lysine residue, and it was not found here.

The oxidation of lysine also produces hydroxylysine with a mass addition of 16 Da. The MS/MS spectrum of ion m/z 486.1 (+16 Da) is shown in Figure 4E. The fragments at m/z 300.1 and 371.1 are y_2+16 and y_3+16, respectively. No y_2 and y_3 signals were observed. The presence of y_2+16 and y_3+16 and the absence of y_2 and y_3 fragments indicate that the +16 Da addition was located at His or Lys. Furthermore, the intensity of b_3 fragment at m/z 324.1 was about 3-fold of that of b_3+16 at m/z 339.8. Thus, lysine residue was possibly responsible for about 75% of the +16 Da product, even though quantification by relative intensity of fragment ions in a tandem MS is not reliable.

The hydroxyl and carbonyl groups in the above oxidation products could be located at any carbon except ϵ-carbon on the side chain of lysine. The reaction of hydroxyl radical with aliphatic amines in aqueous solution is strongly pH-dependent.[61,77,78] Under alkaline conditions, the amine group and the α-carbon of aliphatic amine are the primary targets for hydrogen abstraction by hydroxyl radicals. The reaction between hydroxyl with deprotonated amine is nearly diffusion controlled and the rate is about 1 or 2 orders of magnitude larger than that for its protonated counterpart. Under acidic conditions, the amine is protonated, and its strong inductive effect reduces the electron density of the carbon next to it. Thus, the electrophilic hydrogen abstraction by hydroxyl radical is unfavorable and more likely to take place from carbons further away from the ion.

The dose−response of various oxidation products of the DAHK peptide with exposure time is illustrated in Figure 4F. The amount of oxidized lysine was estimated by the sum of intensity of +14 Da and 75% of that of the +16 Da signals, while the amount of oxidized histidine with +16 Da mass addition was estimated as 25% of that of +16 signal. The rate constants of each modification obtained from the nonlinear regression are presented at Table 2. Aspartic acid was the primary oxidation product of histidine. The conversion to aspartic acid from histidine exhibited the highest rate constant of 12.2 s^{-1}, which is about 8 times that of 2-oxohistidine (+16 Da). Radiolysis of histidine also leads to the formation of −10 and +5 Da products with a rate constant of 4.7 and 6.4 s^{-1}, respectively. Therefore, radiolysis of His generates oxidation products mainly through the opening of imidazole ring. Meanwhile, lysine residue was also oxidized with a rate constant of 10.4 s^{-1}, which was 2−3 times lower than the total oxidation that was seen for histidine in this peptide. As seen in the analysis of DSPDR, the sum of the rates of appearance of oxidized products equals the rate of loss of the unmodified peptide.

(77) Simiä, M.; Neta, P.; Hayon, E. *Int. J. Radiat. Phys. Chem*. **1971**, *3* (3), 309−20.
(78) Neta, P.; Fessenden, R. W. *J. Phys. Chem*. **1971**, *75*, 738−48.

CONCLUSION

All three basic amino acid residues are susceptible to radiolytic oxidization by γ-rays or synchrotron X-rays. These residues, particularly Arg and Lys, are preferentially located at protein surfaces and are frequently involved in protein interactions, making these residues quite valuable for mapping protein surfaces and for probing protein−ligand interactions using radiolytic footprinting. Oxidation of arginine results in a primary product with characteristic mass reduction of 43 Da and two minor products with mass additions of 14 and 16 Da. Arginine residues accumulate stable oxidation products rapidly as compared to phenylalanine and proline, which have been previously demonstrated to be useful footprinting probes. Histidine is oxidized by radiolysis to give a mixture of products with characteristic mass changes of −22, −10, +5, and +16 Da through oxidative opening and addition of imidazole ring. Lysine is also quite susceptible to radiolytic oxidation and is either converted to hydroxylysine or carbonylysine but at a rate slower than histidine. We demonstrate how these residues can be utilized in future footprinting experiments to probe protein structure. The eight residues we have used in the past are excellent probes for examining the burial of hydrophobic groups in the formation of protein−ligand complexes. The basic side-chain probes identified here can analyze protein−ligand interfaces that are driven by charge−charge interactions as well.

ACKNOWLEDGMENT

This research is supported in part by The Biomedical Technology Centers Program of the National Institute for Biomedical Imaging and Bioengineering (P41-EB-01979) and the Innovative Molecular Analysis Technologies Program of the National Cancer Institute (R33-CA-83179).

Received for review September 19, 2003. Accepted October 2, 2003.

AC035104H